

# Screen and stencil printed graphene heat spreaders on printed circuit boards for lowering of light emitting diode temperatures

Downloaded from: https://research.chalmers.se, 2025-11-04 19:35 UTC

Citation for the original published paper (version of record):

Kaindl, R., Dergez, D., Gupta, T. et al (2025). Screen and stencil printed graphene heat spreaders on printed circuit boards for lowering of

light emitting diode temperatures. Surface and Coatings Technology, 517.

http://dx.doi.org/10.1016/j.surfcoat.2025.132821

N.B. When citing this work, cite the original published paper.

research.chalmers.se offers the possibility of retrieving research publications produced at Chalmers University of Technology. It covers all kind of research output: articles, dissertations, conference papers, reports etc. since 2004. research.chalmers.se is administrated and maintained by Chalmers Library

ELSEVIER

Contents lists available at ScienceDirect

### Surface & Coatings Technology

journal homepage: www.elsevier.com/locate/surfcoat



## Screen and stencil printed graphene heat spreaders on printed circuit boards for lowering of light emitting diode temperatures\*

Reinhard Kaindl<sup>a,\*</sup>, David Dergez<sup>b</sup>, Tushar Gupta<sup>c</sup>, Songfeng Pei<sup>e</sup>, Peng-Xiang Hou<sup>e</sup>, Jinhong Du<sup>e</sup>, Chang Liu<sup>e</sup>, Bernhard Fickl<sup>c</sup>, Martin Nastran<sup>c</sup>, Ya Liu<sup>f</sup>, Alexander Blümel<sup>d</sup>, Dominik Eder<sup>c</sup>, Johan Liu<sup>f</sup>, Wencai Ren<sup>e</sup>, Paul Hartmann<sup>a,d</sup>, Wolfgang Waldhauser<sup>a</sup>, Dietmar Kieslinger<sup>b</sup>, Bernhard C. Bayer<sup>c,g,\*\*</sup>

- <sup>a</sup> Joanneum Research, Materials-Institute for Sensors, Photonics and Manufacturing Technologies, Leobner Str. 94a, A-8712, Niklasdorf, Austria
- <sup>b</sup> ZKW Elektronik GmbH, Samuel-Morse-Str. 18, A-2700, Wiener Neustadt, Austria
- <sup>c</sup> Technische Universität Wien (TU Wien), Institute of Materials Chemistry, Getreidemarkt 9/165, A-1060, Vienna, Austria
- d Joanneum Research, Materials-Institute for Sensors, Photonics and Manufacturing Technologies, Franz-Pichler-Str. 30, A-8160, Weiz, Austria
- e Shenyang National Laboratory for Materials Science, Institute of Metal Research, Chinese Academy of Sciences, Shenyang, 110016, PR China
- f Electronics Materials and Systems Laboratory, Department of Microtechnology and Nanoscience (MC2), Chalmers University of Technology, SE-412 96, Göteborg, Sweden
- g University of Vienna, Faculty of Physics, Boltzmanngasse 5, A-1090 Vienna, Austria

#### ARTICLE INFO

Keywords: Graphene Screen printing Stencil printing Light emitting diodes Heat spreaders

#### ABSTRACT

Continuously higher integration levels in (opto-)electronics require new solutions and materials for thermal management of excess heat. Here we investigate the integration of graphene-based heat spreader films with printed circuit board (PCB) assembled, high-power light emitting diodes (LEDs), as used in modern automotive lighting, using industrially highly scalable screen printing and stencil printing of the graphene-based films. We compare screen/stencil printing of graphene heat spreaders on the PCBs from archetypical water- and ester-based inks and characterize the resulting graphene heat spreaders with respect to printing fidelity and resolution, film microstructure, electrical and thermal properties and their performance in lowering LED temperatures during LED operation. Importantly, we use only comparatively low graphene film curing temperatures (150 °C) that are compatible with industrial PCB/surface-mounted-device (SMD) LED integration processes. We find that screen-printed, ester-based graphene heat spreaders result in a modest reduction of LED temperature during operation of on average  $-2~{\rm K}$  with a maximum reduction of  $-4~{\rm K}$ . Generally, our work establishes the feasibility of scalable screen and stencil printing for integration of graphene films with state-of-the-art PCB/SMD assemblies.

#### 1. Introduction

Continuous miniaturization and ever higher integration densities pervade all aspects of (opto-)electronics incl. solid state lighting technology. In particular high power light emitting diodes (LEDs) are currently being integrated at increasing areal densities to facilitate new functionalities such as smart or adaptive lighting [1,2]. Increased integration of LEDs is however associated with the requirement to efficiently distribute the excess heat from the high density, high power LEDs' operation. This is necessary since LEDs inherently suffer from limited

light output and shortened lifetime when operated at elevated junction temperatures [3,4]. Therefore efficient solutions for thermal management of integrated LEDs incl. heat sink and heat spreader materials are highly sought after [5–9].

Graphene is a  $\mathrm{sp}^2$ -bonded monolayer of carbon. For isolated, high-quality monolayer graphene crystals record thermal conductivity ( $\sim$ 5000 W/mK), that surpasses diamond and copper, has been reported [10,11]. Consequently graphene is a currently highly investigated building block for next-generation thermal management solutions [10,11]. Key requirement for use of graphene and graphene-based films

 $<sup>^{\</sup>star}$  This article is part of a Special issue entitled: 'PSE 2024' published in Surface & Coatings Technology.

<sup>\*</sup> Corresponding author.

<sup>\*\*</sup> Correspondence to: B.C. Bayer, Technische Universität Wien (TU Wien), Institute of Materials Chemistry, Getreidemarkt 9/165, A-1060, Vienna, Austria. E-mail addresses: reinhard.kaindl@joanneum.at (R. Kaindl), bernhard.bayer-skoff@tuwien.ac.at (B.C. Bayer).

in thermal management in (opto-)electronics is however the need for scalable fabrication routes for graphene-based heat spreaders and thermal interface materials (TIMs) [10,11]. While graphene's record thermal conductivity has been measured on isolated, atomically-thin monolayers, actual device integration for thermal management currently focusses on µm-thick graphene-based films which are assembled from graphene flake building blocks [10]. For such films, thermal conductivities are drastically reduced (to a few to tens of W/mK) [10] compared to the isolated monolayers due to introduction of interflake junction interfaces and scattering pathways [10,11]. These graphenebased films' thermal conductivities are however nevertheless still high enough to make them interesting for thermal management applications [10] such as heat spreaders in high-power LEDs [8,9,12-28], in particular since graphene-based films can offer additional advantages over competing materials incl. mechanical stability and flexibility, chemical stability, low weight, potentially very low cost and optical translucence, and lack of environmental and health concerns [10]. Consequently, graphene-based heat spreaders have been integrated into LEDs at various device levels [8] incl. packaging [9,12-18], on chip [19-22], phosphor layer [23–26] and extraneous cooling [27,28].

For fabrication and device integration of graphene-based films, various potentially scalable fabrication routes are being investigated [10]. In particular for LED integration processes, printing techniques are promising. For instance, stencil printing is a well-established standard process in surface-mounted-device (SMD) production flows for solder paste printing [29] and jet dispensing is for various tasks also finding widespread adoption [30]. These techniques allow cost-effective highvolume manufacturing of printed circuit board (PCB) assemblies. To date a lot of work on printing of graphene and graphene-based films has focused on additive manufacturing techniques like inkjet or aerosol jet printing [31-33]. Compared to the specifications of these novel additive manufacturing techniques in terms of required ink viscosity, limited solid carbon content, limited throughput and higher cost [31–33], more traditional but also more scalable and inexpensive printing techniques are screen and stencil printing [34-37]. Typically in screen printing, inks of suitable viscosity ( $\sim$ 10,000 cP) are pressed on patterned meshes ("screen") with the help of a so called "squeegee" in order to obtain the predesigned pattern of interest on top of various substrates [34]. Stencil printing is a related printing technique in which no mesh is used but the ink is pressed onto the substrate directly through templating stencils [38]. Screen printing allows very high versatility in possible patterns but mesh clogging can become a problem. For stencil printing, clogging is not an issue however geometry of printing patterns is restricted (e.g., isolated (inverse) "islands" are difficult to achieve in stencils) [38]. Both screen and stencil printing are established technologies in state-of-theart (opto-)electronics manufacturing incl. high-power LED manufacture. Despite this, to date research on graphene printing has somewhat focussed on more exotic inkjet and aerosol jet printing [31-33]. In particular only very little work has employed screen and stencil printing of graphene-films as components in realistic (SMD) device demonstrators [34-37], let alone for graphene heat spreader LED integration using screen or stencil printing.

Towards filling this gap, we here integrate graphene-based film heat spreaders via screen and stencil printing with real-world surface-mount PCB-mounted [39] state-of-the-art high-power LEDs, as used in modern automotive lighting [40,41]. We compare screen printing and stencil printing from archetypical water- and ester-based inks and characterize the resulting graphene heat spreaders in terms of printing fidelity, microstructure, electrical transport and their performance in lowering LED temperatures during operation. In particular, we ensure to only use curing temperatures at comparatively [10] low 150 °C that are compatible with industrial PCB/SMD LED integration processes. Notably, we find that application of screen-printed, ester-based graphene heat spreader films on the PCBs results in a modest reduction of LED temperature during operation of -2 K to -4 K. In a wider context, our work shows the feasibility of using screen and stencil printing for

integration of graphene films with state-of-the-art PCB/SMD stacks.

#### 2. Results and discussion

Fig. 1 shows the device layout for our graphene heat spreaders. In Fig. 1a the device layout without a heat spreader is shown, in which a surface-mount LED (OSLON® Compact CL) is soldered onto the electroless nickel immersion gold (ENIG) or immersion tin (ImmSn) plated copper solder pads spanning across the isolation gap (air) on the PCB (FR4) [39]. In Fig. 1b the same assembly is used with the addition of a printed graphene heat spreader film that spans from the solder pads over a short region of insulting laminate (with low thermal conductivity) to the copper area adjacent to the LED. In this layout it is hypothesized that in particular via the graphene heat spreader "tongues" from the solder pads over the insulting laminates to the adjacent copper areas additional efficient lateral heat transport pathways are established, that can spread heat outwards from the LED into the PCB and subsequently the heat sink onto which such PCBs are mounted on [42]. In this concept, via these additional heat transport pathways the temperature of the LEDs under operation are envisioned to be reduced.

In Fig. 2 we compare typical optical micrographs for screen printing (180 mesh) and stencil printing of graphene heat spreader films (as illustrated in Fig. 1b) directly on PCBs (before LEDs are manually soldered onto the copper solder pads) from a water-based ink and an esterbased ink. Such screen and stencil printing of graphene heat spreader films directly onto PCBs has to date not been investigated in the literature on graphene heat spreader LED integration [8,9,12-28]. For the water-based ink, we used polyvinylpyrrolidone (PVP) as the surfactant and sodium polyacrylate (SPAA) as the resin. Typically, 20 g graphene powder was firstly dispersed in 1 L PVP/water solution (1 %) with ultrasonication for 1 h. Then the mixture was centrifuged at a relative centrifugal force (RCF) of 5000 g for 30 min to remove extra water, and a graphene paste with a solid content of  $\sim 15$  % was collected from the bottom of the centrifuge bottles. 100 g of graphene paste was mixed with 30 g 0.5 % sodium polyacrylate/water solution and 20 g glycerol. The mixture was milled with a three-roller grinding miller to get the waterbased ink with fineness lower than 10  $\mu m$ . This results in an ink with viscosity of ~8000 cP. The ester-based ink is synthesized using aliphatic dibasic esters (DBE, Dupont) as solvent and vinyl chloride-vinyl acetate copolymer (VCVA, Wacker VINNOL E22/48A) as the resin. Typically, 20 g graphene powder was firstly dispersed in 300 g DBE with highshear disperser (Fluko FA25), then 50 g VCVA/DBE solution containing 30 g VCVA was mixed into the graphene/DBE dispersion. The mixture was milled with a three-roller grinding miller to get the esterbased ink with fineness lower than 10 µm, resulting in a viscosity of ~15,000 cP. Printing is undertaken on a desktop prototype printing setup with custom-built silk screen and stainless-steel stencil. After printing, graphene films have been cured under atmospheric conditions in an oven at 150 °C for 5 min before LEDs and other components were manually placed and reflow soldered (using a heating plate and SAC305 solder paste) onto the contact pads of the PCB. These curing conditions are based on industrial PCB/SMD LED-integration process flows of the industrial partner in this study to ensure eventual compatibility with the industrial process lines. Higher curing temperatures or longer curing would limit compatibility with the industrial integration processes. We note that the here employed curing conditions are very mild (150 °C, 5 min) in comparison to often employed much higher temperature treatments for curing of graphene-based heat spreaders and TIMs [10]. Further details on materials and methods can be found in the Supplementary Information.

The optical micrographs in Fig. 2a reveal that water-based ink and screen printing resulted in good and homogeneous transfer of desired features onto the PCB, incl. well deposited graphene heat spreader "tongues". In particular no graphene film has deposited over the isolation gap between cathode and anode contact for the LEDs. Such graphene film deposition over the isolation gap is highly undesirable as it

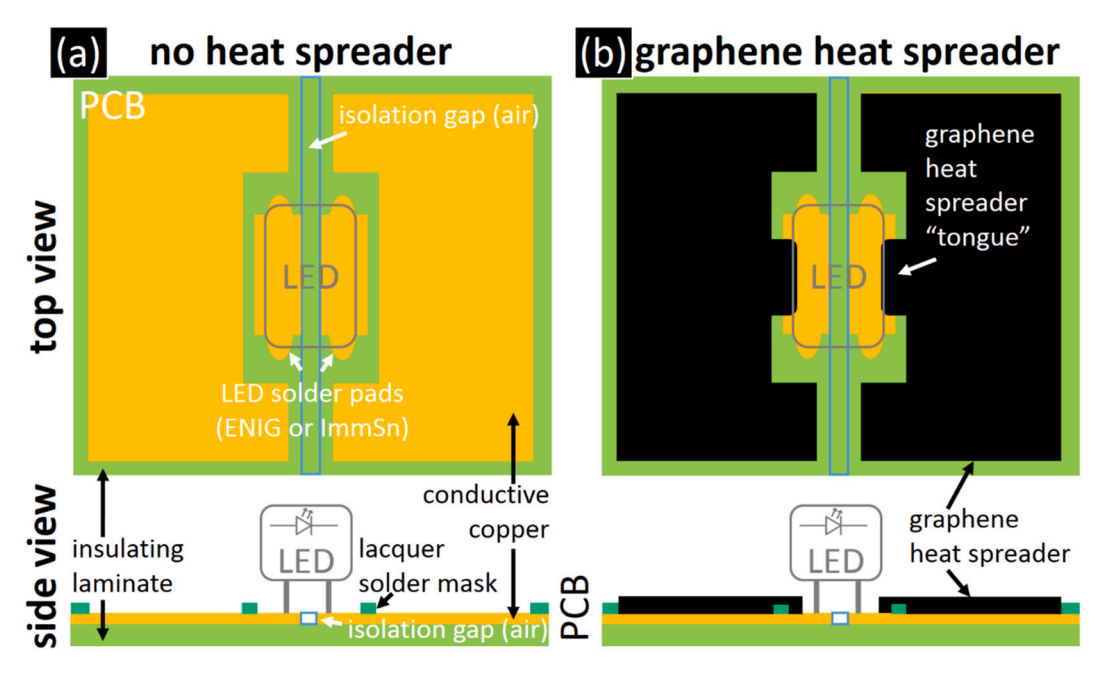


Fig. 1. (a) Schematic illustrations of PCB layout and LED mounting without (a) and with (b) the screen/stencil printed graphene heat spreader in top view (top) and side view (bottom).

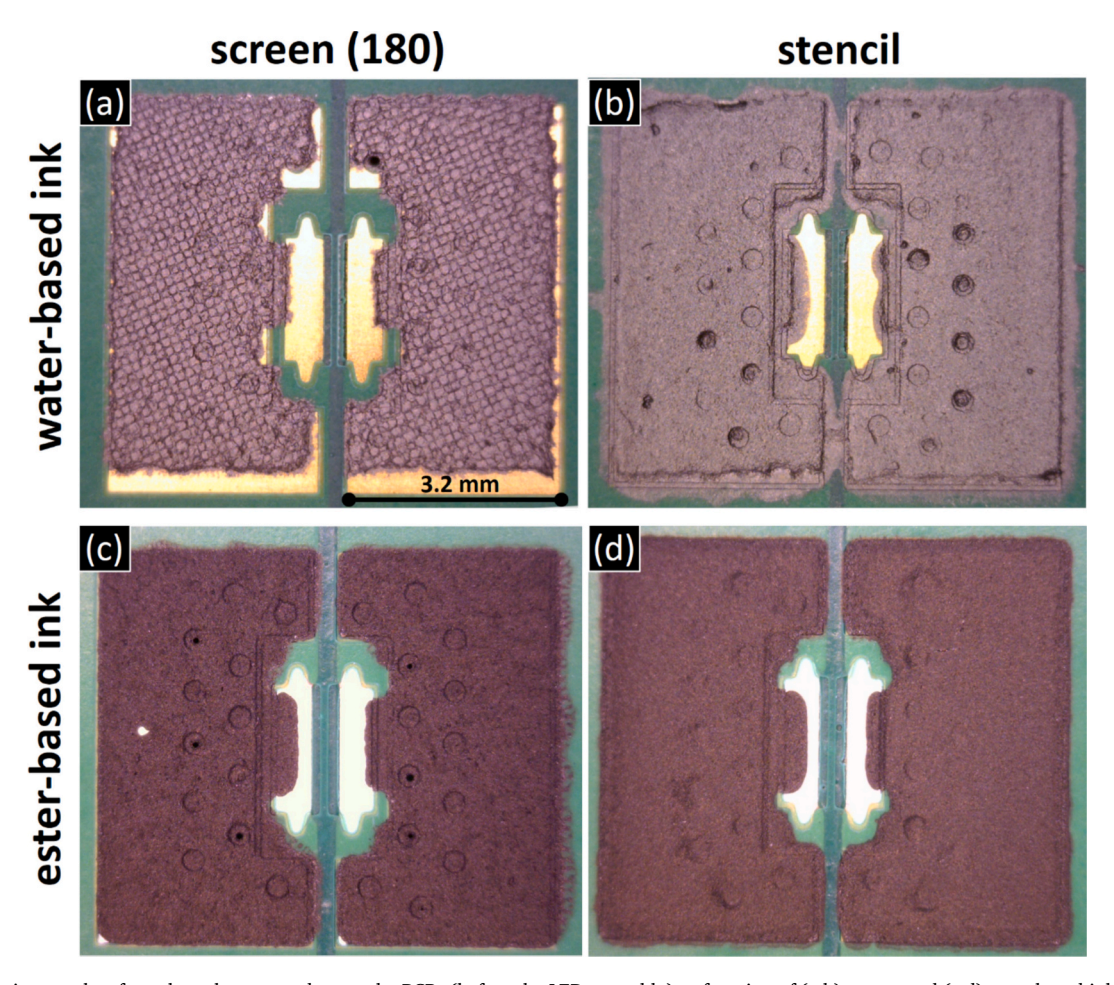


Fig. 2. Optical micrographs of graphene heat spreaders on the PCBs (before the LED assembly) as function of (a,b) water- and (c,d) ester-based ink usage and (a,c) screen and (b,d) stencil printing.

would short-circuit the LED and thus render the device inoperable. A partial transfer of mesh features is observed in the deposits in Fig. 2a, evident by the mesh appearance of the graphene-based film surface morphology.

In contrast to the high fidelity of printed features for water-based ink with screen printing, the results for water-based ink with stencil printing in Fig. 2b show significant lateral flow of the graphene deposits, rendering the printing quality from this combination inferior. In particular, we observe that the graphene heat spreader "tongues" are rather undefined. In addition, undesired, partial graphene film deposition across the isolation gap is clearly observable. A smooth surface morphology of the graphene deposits is observed (in keeping with absence of a mesh in stencil printing).

Fig. 2c shows the results of screen printing with the ester-based ink. Good fidelity of printed features and only very little lateral flow is observed. Heat spreader "tongues" are well developed and no graphene deposition on the isolation gap is observed. In comparison to the water-based ink, the surface morphology from screen printing with the ester-based ink is comparatively smooth with no mesh feature transfer visible in the optical micrographs in Fig. 2c.

Fig. 2d shows the results of stencil printing with the ester-based ink. Fidelity of printed features is high with well-developed "tongues" and no graphene deposition over the isolation gap. The surface of the graphene film appears smooth.

Across our depositions, we also compare two different PCB copper surface finishes, namely electroless nickel immersion gold (ENIG) and immersion tin (ImmSn) [39]. Notably, when comparing the same printing conditions on both surface finishes we find no significant differences in printing results between ENIG and ImmSn PCBs. Also printing directly on the laminate of the PCB yields printing results of similar definition (not shown), suggesting that graphene screen and stencil printing on ENIG, ImmSn and PCB laminate is feasible.

In terms of clogging, we find that with both water- and ester-based inks the screen printing results with the 180 mesh degrade after  $\sim 3$  iterations due to clogging. The meshes can however readily be cleaned from both inks, restoring initial printing quality as in Fig. 2. For stencil printing clogging is no issue.

Fig. 2 indicates some advantages of the ester-based ink over the water-based ink for both screen and stencil printing: For screen printing the water-based ink suffered from unplanned impression of mesh features on the graphene deposits (Fig. 2a) and for stencil printing massive lateral flow drastically limited printing fidelity and resolution for the water-based ink (Fig. 2b). Both shortcoming were not detected for the ester-based ink (Fig. 2c,d), suggesting that the ester-based ink may be more suitable for the here studied integration process flow. We attribute

the lack of significant lateral flow of the ester-based ink to its higher viscosity ( $\sim$ 15,000 cP) compared to the water-based ink ( $\sim$ 8000 cP).

Fig. 3 investigates the microstructure of the graphene deposits from water-based (Fig. 3a) and ester-based ink (Fig. 3b) by optical microscopy and SEM. Via Dektak profilometer measurements over film edge steps we measure graphene film thickness after drying to  $\sim 10 \mu m$  for the screen printed films (from mesh thickness  $\sim 45 \, \mu m$ ) and to  $\sim 20 \, \mu m$  for the stencil printed films (from stencil thickness  $\sim$ 80 µm), respectively. Average roughness ( $R_a$ ) values are measured to  $\sim$ 4  $\mu m$  for the screen printed and  $\sim 3~\mu m$  for the stencil printed films, respectively. We also measure the electrical sheet resistance of the films using a multiplecontact two-terminal transmission line model (TLM) method [33,43] which facilitates an order of magnitude estimation of sheet resistance (we estimate relative uncertainty in our sheet resistance measurement to ~20 % [33]). To this end, test graphene films are deposited onto insulting laminate sections of the PCBs (i.e. no conductive ENIG and ImmSn regions under the graphene films. Sheet resistance of laminate >2 M $\Omega/\Box$ .). Likewise, we measure in-plane thermal conductivity of screen-printed, quasi-freestanding films from the two inks by a Joule heating method (see Supporting Information) [44–46]. We note that this approach cannot yield exact thermal conductivities for all sampled conditions on the PCBs but generally allows an order-of-magnitude assessment of thermal conductivities and would thus highlight severe differences between films from the two inks.

For the water-based, screen-printed films, higher magnification optical microscopy (Fig. 3a, left) confirms the mesh impressions, consistent with Fig. 2a. SEM imaging (Fig. 3a, middle) shows that the water-based graphene film has a compact, dense appearance and predominantly consists of flakes with lateral dimensions on the order of few um. In cross-sectional SEM images in Supplementary Fig. 1, the graphene flakes appear predominantly oriented in the film with their basal planes parallel to the substrate. Corresponding Raman spectroscopy in Fig. 3a, right reveals a 2D/G intensity ratio (G peak at ~1580 cm<sup>-1</sup>; 2D at  $\sim$ 2707 cm<sup>-1</sup>) of  $\sim$ 0.37 which suggests that these flakes are graphene nanoplatelets or few- to multi-layer graphene crystals [47,48]. Notably, we also find a sizable defect-related D peak (at  $\sim 1345 \text{ cm}^{-1}$ ) in the Raman data with a D/G ratio of  $\sim$ 0.21 for the water-based film. This is comparable to crystalline defect levels as in prior reports of screen printed graphene [34]. Additionally, the SEM data in Fig. 3a, middle reveals also particulate agglomerates of tens to hundreds nm large particles that are adhering to the graphene flakes. We attribute these particles to the PVP and SPAA from water-based ink preparation. For the water-based film we measure a sheet resistance of  $\sim 3.5 \ \Omega/\square$ , which translates to a resistivity of  $\sim 3.5 \times 10^{-5} \, \Omega m$  and a conductivity of  $\sim 3 \times 10^{-5} \, \Omega m$  $10^4$  S/m, respectively. An in-plane thermal conductivity of ~5 W/mK is

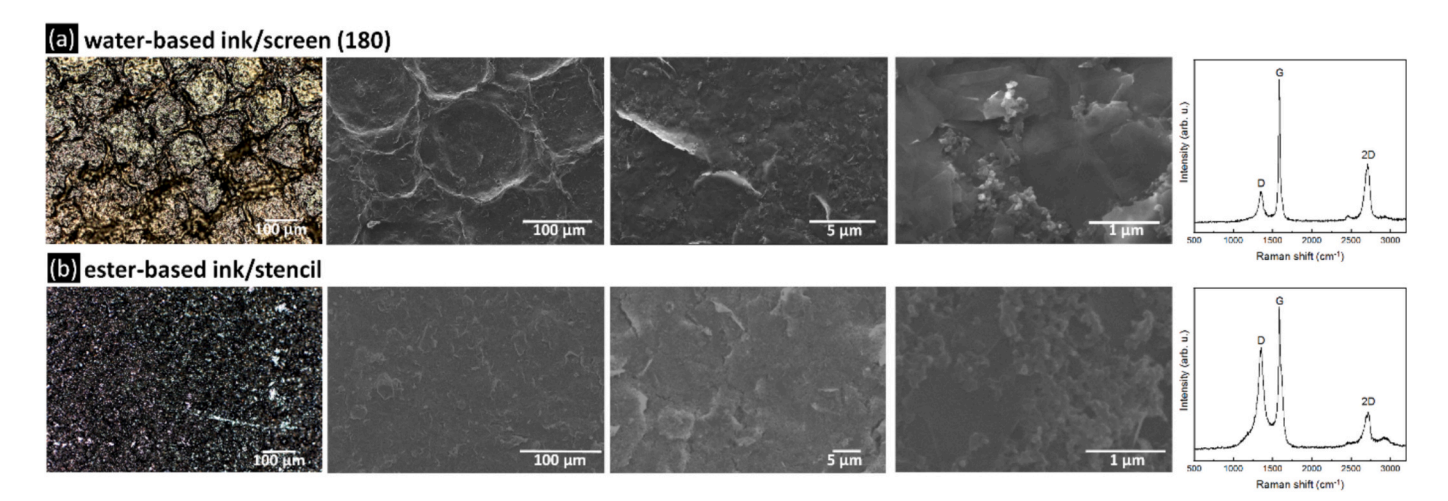


Fig. 3. Optical micrographs (left), SEM images at various magnifications (middle) and Raman spectra (right) for (a) water-based screen printed and (b) ester-based stencil printed graphene films on PCB substrate.

measured for a film from the water-based ink.

Fig. 3b shows similar optical microscopy, SEM and Raman data for a stencil printed film from the ester-based ink. In keeping with Fig. 2d, we find a smooth surface morphology in Fig. 3b, right. In terms of microstructure analysis, the SEM data (Fig. 3b, middle) reveals a compact film consisting of few-layer graphene flakes with predominant orientation of basal plane parallel to the substrate (Supplementary Fig. 1) which are decorated with particle agglomerates, ascribed to VCVA resin, in the ester-based film. Raman spectroscopy (Fig. 3b, right) with a 2D/G  $\sim$  0.24 and an even more appreciable defect level (D/G  $\sim$  0.72) suggests a nature of graphene nanoplatelets or multi-layer graphene for the esterbased film. [47,48] For the ester-based film we measure a sheet resistance of  $\sim$ 0.8  $\Omega$ / $_$ , which corresponds to a resistivity of  $\sim$ 1.5  $\times$  10 $^{-5}$   $\Omega$ m and a conductivity of  $\sim$ 6  $\times$  10 $^4$  S/m, respectively. An in-plane thermal conductivity of  $\sim$ 5 W/mK is measured for a film from the ester-based ink.

The data in Fig. 3 together with the TLM electrical measurements and in-plane thermal conductivities indicates that microstructures of water-based and ester-based inks are similar. Defect levels and sheet resistance from both our inks are on par with prior reports for screen-printed graphene films [34,35,49–52]. We attribute the defect levels detected in Raman spectroscopy to the edges of the graphene flakes [53] as well as defects in the basal plane arising during the production process, in particular the three-roller grinding miller process. The measured thermal conductivities are moderate and consistent with similar graphene heat spreader films that also underwent only such low temperature curing [10].

After screen/stencil printing and curing, LEDs are manually assembled onto the graphene heat spreader integrated PCBs. This is done via manual soldering of the LED contacts onto the copper solder pads. An exemplary, completed LED/PCB structure incl. a graphene heat spreader is depicted in the optical micrograph in Fig. 4a. We find that soldering can be readily achieved if solder pads are free from graphene deposits, which should be the case for high fidelity printed features according to our planned device layout with the graphene heat spreader "tongues" leaving enough room on copper solder pads for LED contact soldering (compare layout sketch in Fig. 1b and actual realization in Fig. 4a). Thus

assembled LED/graphene heat spreader/PCB structures are then tested for functionality over multiple LED assemblies. We find that LEDs in our test structures with the graphene heat spreaders are fully operational, as depicted in the photo of an array of multiple LED/graphene heat spreaders on a PCB (Fig. 4b) that is successfully switched on with all LEDs fully illuminating. The data in Fig. 4 thereby indicates that the here investigated graphene heat spreader printing is fully compatible with the fabrication flow and operation of modern LED/PCB assemblies, which to date had not been investigated in the literature on graphene heat spreader integration with LEDs [8,9,12–28].

Finally, we measure via an infra-red (IR) camera the temperature of the LEDs in on-state, as shown in an example in Fig. 5 (assembled PCBs mounted onto an aluminium metal heat sink). The LED string is driven by a forward current of 700 mA, and temperatures are measured after an equilibration time of 10 min, whereby temperatures are always measured via hottest spot on the individual LED phosphor layer. Stated temperatures are averaged over 11 LEDs per sample condition and stated uncertainties are standard deviations. We assess the thermal device performance with vs. without the graphene heat spreader "tongues" by directly measuring the temperatures via IR camera of the surfacemounted LEDs' phosphor layers that are mounted over/next the graphene heat spreaders which itself are on the PCB level below the LEDs (layout Fig. 1, photo in Fig. 4) [54]. The advantage of this approach is that the LEDs therefore do not have any graphene coating applied on top. Therefore, the emissivities of the LEDs' phosphor layers remain unaltered and are not expected to change for conditions with vs. without graphene heat spreader tongues, as emission in all cases comes from the same type of phosphor layer of the LEDs unhindered. This allows us to directly compare LED temperatures (without having to correct for graphene-induced changes for emissivities) for LED/graphene heat spreader/PCB assemblies, benchmarked against the same LED/PCB assemblies but without an extraneous graphene heat spreader. Thereby we can disentangle the effect of the graphene heat spreaders on LED temperature under operation and thus measure a directly LED-integrationand applicant-relevant performance indicator (maximum LED temperature) for our graphene heat spreader films [15,16,18].

Interestingly, we find no temperature reduction effect by the

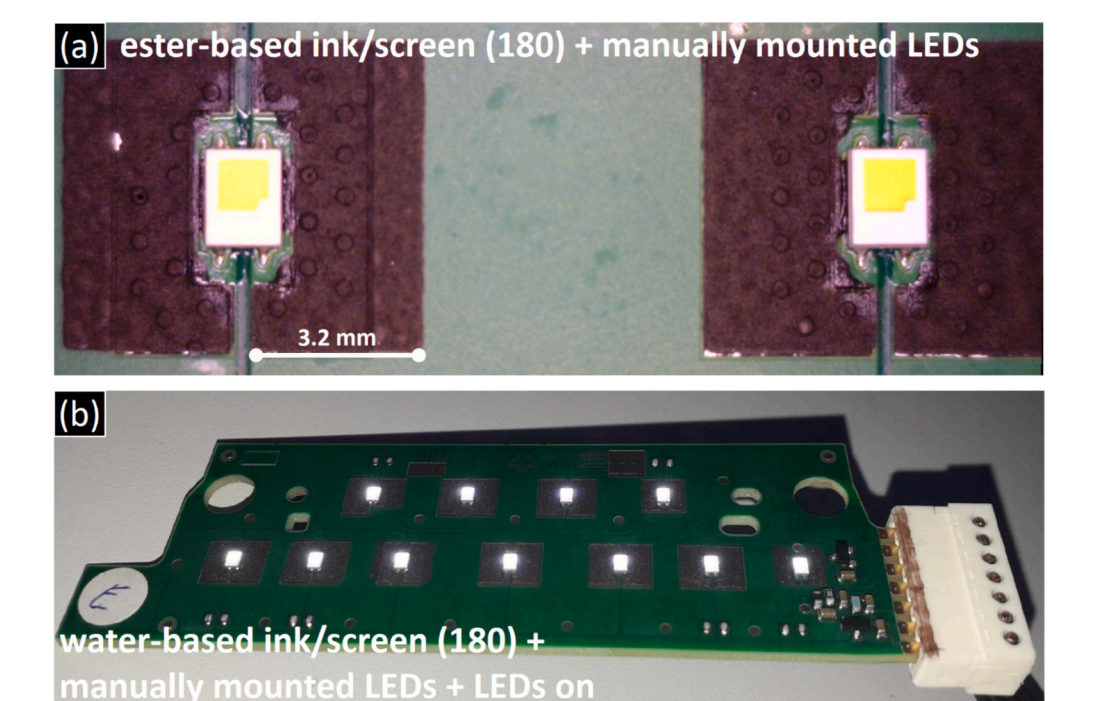


Fig. 4. (a) Optical micrograph of graphene heat spreaders on the PCBs with the LEDs mounted. (b) Illuminating string of LEDs with integrated water-based screen-printed graphene heat spreaders driven at 700 mA.

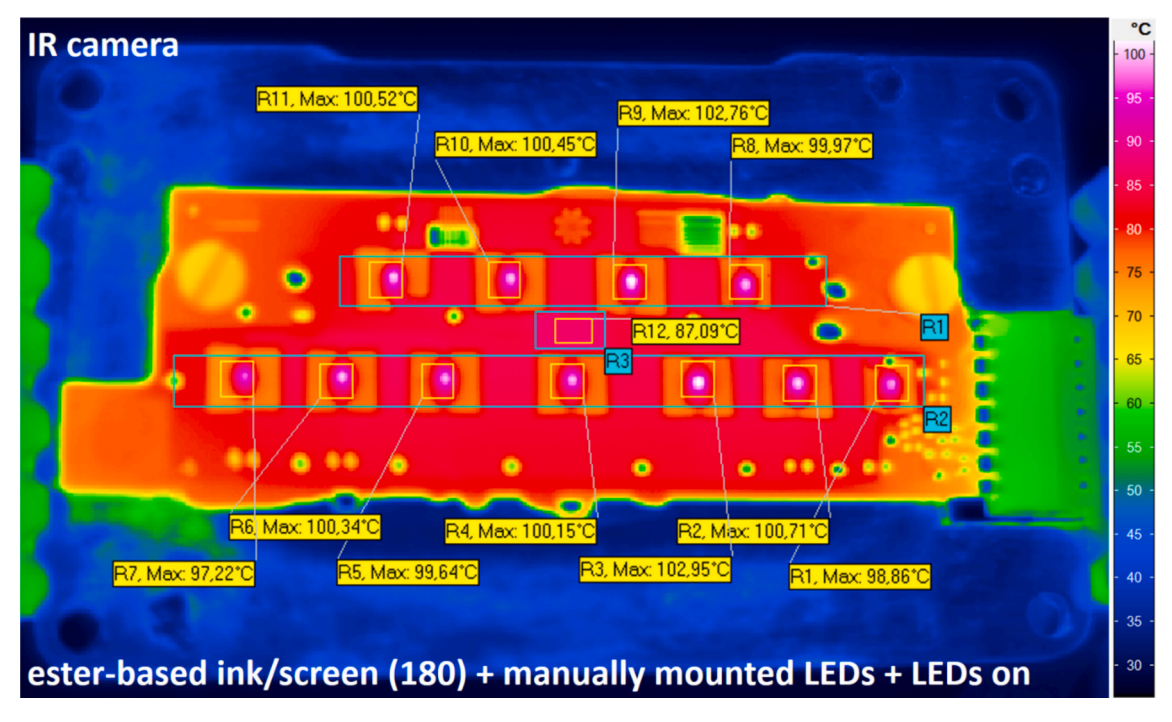


Fig. 5. (a) IR camera image of an illuminating string of LEDs with integrated ester-based screen-printed graphene heat spreaders driven at 700 mA. Maximum temperatures of the individual LEDs are indicated.

application of the graphene heat spreaders for the water-based/screen printed, water-based/stencil printed and ester-based/stencil printed films. We find however a modest reduction in LED temperatures under operation for the ester-based/screen printed graphene heat spreaders (Fig. 5) of on average  $-2.0~\rm K$  ( $\pm~0.9~\rm K$ , standard deviation) with a maximum value of temperature reduction by  $-4.0~\rm K$ .

From an application perspective, the obtained heat spreader performance is only modest and will require further optimization (e.g., to heat spreader layout design). Also higher curing temperatures would likely improve thermal performance [10] but are hard to implement when wanting to ensure compatibility with industrial PCB/SMD LED integration processes. Beyond final heat spreader performance, on a materials integration process technology level, our study however particularly demonstrates that screen and stencil printing can be readily utilized for integration of graphene films on PCBs, while still allowing subsequent functional mounting of SMD devices, as here demonstrated for SMD LEDs on PCBs.

#### 3. Conclusions

In summary, we here investigated integration of graphene-based heat spreader films with PCB-mounted high-power LEDs as used in modern automotive lighting. To this end, graphene heat spreader films were deposited using industrially compatible screen and stencil printing onto the PCBs before LED assembly. We compared water- and esterbased inks and characterized the resulting graphene heat spreaders regarding printing fidelity, film microstructure and electrical and thermal properties. We use only comparatively low curing temperatures (150 °C) to ensure compatibility with industrial PCB/SMD LED integration processes. Notably, we also tested the graphene heat spreaders' performance in lowering LED temperatures during operation, whereby we found that ester-based, screen-printed graphene heat spreaders resulted in a modest reduction of LED temperature during operation of −2 K to −4 K. Notably, no prior literature on graphene heat spreader and LED integration [8,9,12-28] has before demonstrated such integration of graphene heat spreader films on the PCB level with high-power LEDs using screen or stencil printing, despite the clear industrial merit of both

printing techniques. Our work establishes the feasibility of using screen and stencil printing for integration of graphene films incl. graphene heat spreaders with state-of-the-art, industrially assembled PCB/SMD stacks incl. PCB/LEDs.

#### CRediT authorship contribution statement

Reinhard Kaindl: Writing - review & editing, Supervision, Project administration, Methodology, Investigation, Funding acquisition, Formal analysis, Data curation, Conceptualization. David Dergez: Writing - review & editing, Methodology, Investigation, Formal analysis, Data curation, Conceptualization. Tushar Gupta: Investigation. Songfeng Pei: Investigation. Peng-Xiang Hou: Investigation. Jinhong Du: Investigation. Chang Liu: Investigation. Bernhard Fickl: Investigation. Martin Nastran: Investigation. Ya Liu: Investigation. Alexander Blümel: Investigation. Dominik Eder: Investigation. Johan Liu: Investigation. Wencai Ren: Supervision, Project administration, Funding acquisition, Conceptualization. Paul Hartmann: Investigation, Funding acquisition. Wolfgang Waldhauser: Investigation. Dietmar Kieslinger: Project administration, Methodology, Investigation, Funding acquisition, Conceptualization. Bernhard C. Bayer: Writing original draft, Supervision, Project administration, Methodology, Investigation, Funding acquisition, Formal analysis, Data curation, Conceptualization.

#### **Declaration of competing interest**

The authors declare the following financial interests/personal relationships which may be considered as potential competing interests:

Bernhard C. Bayer reports financial support was provided by Austrian Federal Ministry for Climate Action, Environment, Energy, Mobility, Innovation and Technology. Bernhard C. Bayer reports financial support was provided by Austrian Research Promotion Agency (FFG) grant number 857181-GRATEC. Wencai Ren reports financial support was provided by Chinese Academy of Sciences (174321KYSB20160011). If there are other authors, they declare that they have no known competing financial interests or personal

relationships that could have appeared to influence the work reported in this paper.

#### Acknowledgements

We acknowledge funding from the Austrian Federal Ministry for Climate Action, Environment, Energy, Mobility, Innovation and Technology, Austrian Research Promotion Agency (FFG) grant number 857181-GRATEC and the Chinese Academy of Sciences (174321KYSB20160011). We acknowledge the use of facilities at the University Service Centre for Transmission Electron Microscopy (USTEM) and the Analytic Instrumentation Center (AIC) at TU Wien. Y. Liu and J. Liu acknowledge financial support from Area of Advance: Production from Chalmers University of Technology. The authors acknowledge TU Wien Bibliothek for financial support through its Open Access Funding Programme.

#### Appendix A. Supplementary data

Supplementary data to this article can be found online at https://doi.org/10.1016/j.surfcoat.2025.132821.

#### Data availability

Data will be made available on request.

#### References

- [1] X. Long, J. He, J. Zhou, L. Fang, X. Zhou, F. Ren, T. Xu, A review on light-emitting diode based automotive headlamps, Renew. Sustain. Energy Rev. 41 (2015) 29–41.
- [2] L. Wang, J. Ma, P. Su, J. Huang, High-resolution pixel LED headlamps: functional requirement analysis and research progress, Appl. Sci. 11 (2021) 3368.
- [3] S. Ishizaki, H. Kimura, M. Sugimoto, Lifetime estimation of high power white LEDs, J. Light. Vis. Environ. 31 (2007) 11–18.
- [4] X.-X. Wang, L. Jing, Y. Wang, Q. Gao, Q. Sun, The influence of junction temperature variation of LED on the lifetime estimation during accelerated aging test, IEEE Access 7 (2018) 4773–4781.
- [5] P.H. Chen, C.L. Lin, Y. Liu, T.Y. Chung, C.-Y. Liu, Diamond heat spreader layer for high-power thin-GaN light-emitting diodes, IEEE Photon. Technol. Lett. 20 (2008) 045-947
- [6] X. Zhang, M. Chen, Z. Hao, S. Liu, Research on Direct Plated Copper Heat Spreader and Its Thermal Performances for High Power LED Packaging, IEEE, 2013, pp. 1193–1196
- [7] H. Steiner, T. Sauter, M. Schlauf, T. Schalkhammer, R. Führinger, D. Kieslinger, Challenges of In-situ Thermal Characterization of Thin-Film Isolation Layers for Printed Electronics, IEEE, 2018, pp. 803–808.
- [8] M. Hamidnia, Y. Luo, X.D. Wang, Application of micro/nano technology for thermal management of high power LED packaging – a review, Appl. Therm. Eng. 145 (2018) 637–651.
- [9] R. Li, Q. Liu, L. Huang, L. Yin, G. Song, Properties of thermal interface materials and its impact on thermal dissipation and reliability of LED automotive lighting, in: 2018 15th China International Forum on Solid State Lighting: International Forum on Wide Bandgap Semiconductors, IFWS, China (SSLChina, 2018, pp. 1–4.
- [10] Y. Fu, J. Hansson, Y. Liu, S. Chen, A. Zehri, M.K. Samani, N. Wang, Y. Ni, Y. Zhang, Z.-B. Zhang, Q. Wang, M. Li, H. Lu, M. Sledzinska, C.M.S. Torres, S. Volz, A. A. Balandin, X. Xu, J. Liu, Graphene related materials for thermal management, 2D Mater. 7 (2019) 012001.
- [11] T. Ma, Z. Liu, J. Wen, Y. Gao, X. Ren, H. Chen, C. Jin, X.-L. Ma, N. Xu, H.-M. Cheng, W. Ren, Tailoring the thermal and electrical transport properties of graphene films by grain size engineering, Nat. Commun. 8 (2017) 14486.
- [12] T.-J. Hsiao, T. Eyassu, K. Henderson, T. Kim, C.-T. Lin, Monolayer graphene dispersion and radiative cooling for high power LED, Nanotechnology 24 (2013) 395401.
- [13] S. Lee, Y.K. Kim, J. Jang, Long-term stability improvement of light-emitting diode using highly transparent graphene oxide paste, Nanoscale 8 (2016) 17551–17559.
- [14] H. Zhang, Y. Lin, D. Zhang, W. Wang, Y. Xing, J. Lin, H. Hong, C. Li, Graphene Nanosheet/silicone composite with enhanced thermal conductivity and its application in heat dissipation of high-power light-emitting diodes, Curr. Appl. Phys. 16 (2016) 1695–1702.
- [15] H. Cho, et al., Graphene–carbon–metal composite film for a flexible heat sink, ACS Appl Mater Inter 9 (2017) 40801–40809.
- [16] J. Oliva, A.I. Mtz-Enriquez, A.I. Oliva, R. Ochoa-Valiente, C.R. Garcia, Q. Pei, Flexible graphene composites with high thermal conductivity as efficient heat sinks in high-power LEDs, J. Phys. Appl. Phys. 52 (2019) 025103.
  [17] B.D. Ryu, M. Han, K.B. Ko, K.-H. Lee, T.V. Cuong, N. Han, K. Kim, J.H. Ryu, N.-
- [17] B.D. Ryu, M. Han, K.B. Ko, K.-H. Lee, T.V. Cuong, N. Han, K. Kim, J.H. Ryu, N. J. Park, Y. Lim, Reduced thermal resistance of heat sink using graphene oxide decorated with copper nanoparticles, Mater. Res. Bull. 110 (2019) 76–81.

- [18] Q. Sun, J. Liu, Y. Peng, A. Wang, Z. Wu, M. Chen, Effective heat dissipation of highpower LEDs through creation of three-dimensional ceramic substrate with kaolin/ graphene suspension, J. Alloys Compd. 817 (2020) 152779.
- [19] N. Han, E. Jung, M. Han, B.D. Ryu, K.B. Ko, Y.J. Park, T. Cuong, J. Cho, H. Kim, C.-H. Hong, Reduced junction temperature and enhanced performance of high power light-emitting diodes using reduced graphene oxide pattern, J. Phys. Appl. Phys. 48 (2015) 265102.
- [20] M. Han, N. Han, E. Jung, B.D. Ryu, K.B. Ko, T. Viet Cuong, H. Kim, J.K. Kim, C.-H. Hong, Effect of curved graphene oxide in a GaN light-emitting-diode for improving heat dissipation with a patterned sapphire substrate, Semicond. Sci. Technol. 31 (2016) 085010.
- [21] F. Qin, C. Xu, G. Zhu, F. Chen, R. Wang, J. Lu, D. You, X. Wang, W. Zhang, J. Zhao, Brightness improvement in a graphene inserted GaN/ZnO heterojunction light emitting diode, J. Phys. Appl. Phys. 52 (2019) 395104.
- [22] F. Xiong, J. Sun, M.T. Cole, W. Guo, C. Yan, Y. Dong, L. Wang, Z. Du, S. Feng, X. Li, GaN LEDs with in situ synthesized transparent graphene heat-spreading electrodes fabricated by PECVD and penetration etching, J. Mater. Chem. C 10 (2022) 6704\_6804
- [23] G. Anoop, J.R. Rani, J. Lim, M.S. Jang, D.W. Suh, S. Kang, S.C. Jun, J.S. Yoo, Reduced graphene oxide enwrapped phosphors for long-term thermally stable phosphor converted white light emitting diodes, Sci. Rep. 6 (2016) 1–9.
- [24] E. Kim, H.W. Shim, S. Unithrattil, Y.H. Kim, H. Choi, K.-J. Ahn, J.S. Kwak, S. Kim, H. Yoon, W.B. Im, Effective heat dissipation from color-converting plates in highpower white light emitting diodes by transparent graphene wrapping, ACS Nano 10 (2016) 238–245.
- [25] Y.-H. Song, E.K. Ji, S.-H. Bak, Y.N. Kim, D.B. Lee, M.K. Jung, B.W. Jeong, D.-H. Yoon, New design of hybrid remote phosphor with single-layer graphene for application in high-power LEDs, Chem. Eng. J. 287 (2016) 511–515.
- [26] Z. Chen, C. Hou, Q. Zhang, Y. Li, H. Wang, Reinforced heat dissipation by simple graphene coating for phosphor-in-glass applied in high-power LED, J. Alloys Compd. 774 (2019) 954–961.
- [27] K.K. Lay, B.M.Y. Cheong, W.L. Tong, M.K. Tan, Y.M. Hung, Effective micro-spray cooling for light-emitting diode with graphene nanoporous layers, Nanotechnology 28 (2017) 164003.
- [28] J.S. Gan, H. Yu, M.K. Tan, A.K. Soh, H.A. Wu, Y.M. Hung, Performance enhancement of graphene-coated Micro heat pipes for light-emitting diode cooling, Int. J. Heat Mass Transf. 154 (2020) 119687.
- [29] C. Huang, Y. Lin, K. Ying, C. Ku, The solder paste printing process: critical parameters, defect scenarios, specifications, and cost reduction, Soldering & Surface Mount Technology 23 (2011) 211.
- [30] K.-F. Becker, M. Koch, S. Voges, T. Thomas, M. Fliess, J. Bauer, T. Braun, R. Aschenbrenner, M. Schneider-Ramelow, K.-D. Lang, Precision jetting of solder paste–a versatile tool for small volume production, International Microelectronics Assembly and Packaging Society 2014 (2014) 000438–000443.
- [31] E. Jabari, F. Ahmed, F. Liravi, E.B. Secor, L. Lin, E. Toyserkani, 2D printing of graphene: a review, 2D Mater. 6 (2019) 042004.
- [32] L. Ng, G. Hu, R. Howe, X. Zhu, Z. Yang, C.G. Jones, T. Hasan, Printing of Graphene and Related 2D Materials, Springer, 2018.
- [33] R. Kaindl, T. Gupta, A. Blümel, S. Pei, P.-X. Hou, J. Du, C. Liu, P. Patter, K. Popovic, D. Dergez, K. Elibol, E. Schafler, J. Liu, D. Eder, D. Kieslinger, W. Ren, P. Hartmann, W. Waldhauser, B.C. Bayer, Aerosol jet printing of graphene and carbon nanotube patterns on realistically rugged substrates, ACS Omega 6 (2021) 34301–34313.
- [34] P. He, J. Cao, H. Ding, C. Liu, J. Neilson, Z. Li, I.A. Kinloch, B. Derby, Screen-printing of a highly conductive graphene ink for flexible printed electronics, ACS Appl. Mater. Interfaces 11 (2019) 32225–32234.
- [35] K. Jaakkola, V. Ermolov, P. Karagiannidis, S. Hodge, L. Lombardi, X. Zhang, R. Grenman, H. Sandberg, A. Lombardo, A.C. Ferrari, Screen-printed and spray coated graphene-based RFID transponders, 2D Mater. 7 (2019) 015019.
- [36] K. Arapov, E. Rubingh, R. Abbel, J. Laven, G. de With, H. Friedrich, Conductive screen printing inks by gelation of graphene dispersions, Adv. Funct. Mater. 26 (2016) 586–593.
- [37] W.J. Hyun, E.B. Secor, M.C. Hersam, C.D. Frisbie, L.F. Francis, High-resolution patterning of graphene by screen printing with a silicon stencil for highly flexible printed electronics, Adv. Mater. 27 (2015) 109–115.
- [38] R. Kay, M. Desmulliez, A review of stencil printing for microelectronic packaging, Solder, Surf. Mt. Technol. 24 (2012) 38.
- [39] C.F. Coombs Jr., Printed Circuits Handbook, McGraw-Hill Education, 2008.
- [40] J. Bhardwaj, R. Peddada, B. Spinger, Advances in LEDs for Automotive Applications Vol. 9768, International Society for Optics and Photonics, 2016 p 976811.
- [41] J. Wang, Y. Cai, X. Li, X. Zhao, C. Zhang, Design of automotive headlamp with high-power LEDS, Int. J. Automot. Technol. 15 (2014) 673–681.
- [42] A.L. Moore, L. Shi, Emerging challenges and materials for thermal management of electronics, Mater. Today 17 (2014) 163–174.
- [43] D.K. Schroder, Semiconductor Material and Device Characterization, John Wiley & Sons, 2015.
- [44] L. Zhang, G. Zhang, C. Liu, S. Fan, High-density carbon nanotube Buckypapers with superior transport and mechanical properties, Nano Lett. 12 (2012) 4848–4852.
- [45] G. Xin, H. Sun, T. Hu, H.R. Fard, X. Sun, N. Koratkar, T. Borca-Tasciuc, J. Lian, Large-area freestanding graphene paper for superior thermal management, Adv. Mater. 26 (2014) 4521–4526.
- [46] S. Guo, S. Chen, A. Nkansah, A. Zehri, M. Murugesan, Y. Zhang, Y. Zhang, C. Yu, Y. Fu, M. Enmark, J. Chen, X. Wu, W. Yu, J. Liu, Toward ultrahigh thermal conductivity graphene films, 2D Mater. 10 (2022) 014002.

- [47] A.C. Ferrari, Raman spectroscopy of graphene and graphite: disorder, electron-phonon coupling, doping and nonadiabatic effects, Solid State Commun. 143 (2007) 47–57.
- [48] A. Bianco, H.-M. Cheng, T. Enoki, Y. Gogotsi, R.H. Hurt, N. Koratkar, T. Kyotani, M. Monthioux, C.R. Park, J.M.D. Tascon, J. Zhang, All in the graphene family a recommended nomenclature for two-dimensional carbon materials, Carbon 65 (2013) 1–6.
- [49] H. Pang, L. Xu, D.-X. Yan, Z.-M. Li, Conductive polymer composites with segregated structures, Top. Issue Nanocomposites 39 (2014) 1908–1933.
- [50] A.J. Marsden, D.G. Papageorgiou, C. Vallés, A. Liscio, V. Palermo, M.A. Bissett, R. J. Young, I.A. Kinloch, Electrical percolation in Graphene–Polymer composites, 2D Mater. 5 (2018) 032003.
- [51] U. Szeluga, S. Pusz, B. Kumanek, K. Olszowska, A. Kobyliukh, B. Trzebicka, Effect of graphene filler structure on electrical, thermal, mechanical, and fire retardant

- properties of epoxy-graphene nanocomposites a review, Crit. Rev. Solid State Mater. Sci. 46 (2021) 152–187.
- [52] V. Orts Mercadillo, K.C. Chan, M. Caironi, A. Athanassiou, I.A. Kinloch, M. Bissett, P. Cataldi, Electrically conductive 2D material coatings for flexible and stretchable electronics: a comparative review of graphenes and MXenes, Adv. Funct. Mater. 32 (2022) 2204772.
- [53] M. Nastran, P. Peschek, I. Walendzik, J. Rath, B. Fickl, J.S. Schubert, W. Ipsmiller, A. Bartl, G. Mauschitz, G. Szabo, R.A. Wilhelm, J. Schmidt, D. Eder, B.C. Bayer, Liquid phase exfoliation of graphene using ammonia as an easy-to-remove additive in low-boiling organic-water co-solvent suspensions, Commun. Chem. 8 (2025) 161
- [54] C. Yao, G. Leahu, M. Holicky, S. Liu, B. Fenech-Salerno, M.C. Lai, M.C. Larciprete, C. Ducati, G. Divitini, R.L. Voti, C. Sibilia, F. Torrisi, Thermally conductive hexagonal boron nitride/polymer composites for efficient heat transport, Adv. Funct. Mater. 34 (2024) 2405235.